Climate Change and Bias Correction of NOAA's GFDL-GFDL-ESM2M Climate Model for Maximum and Minimum Temperatures in the Southwest Region of Madagascar

MAXWELL Djaffard[1], DONA Victorien Bruno[1], RAKOTOVELO Geoslin[1], RATIARISON Adolphe Andriamanga[2]

[1]*Laboratory of Applied Physics and Renewable Energies, Mahajanga University, Madagascar*
[2]*Laboratory of Atmospheric, Climate and Ocean Dynamics, University of Antananarivo, Madagascar*

ABSTRACT

This article presents the study of temperatures in the southwestern region of Madagascar, delimited by latitudes -21 ° to -26 ° and longitudes 43 ° to 46 °. The study area experienced a significant upward trend for the maximum temperature of 0.022 ° C per year and an overall average increase of 0.23 ° C after the break-up date of 2003. This area can be subdivided into 5 regions relative to the maximum temperature and 3 relative to the minimum temperature. Each region has a specific microclimate towards others.
The GFDL-GFDL-ESM2M climate model of the National Oceanographic and Administration for each region was biased by the debinding method, the quantile-quantile method, and the delta method. The results reveal that one method of bias correction can be adapted for one region but not for another.

Keyword: *temperature, climatological mean, anomaly, trend, Mann-Kendall test, Pettitt test, Principal Component Analysis, climate model, debinding method, quantile-quantile method, delta method, RCP4.5, RCP8.5.*

1. INTRODUCTION

If we compare over a period and a given space, for a given parameter, the average of climate simulations to that of observations, we generally find a fairly good agreement. However, the agreement is not perfect. Not only are there systematic errors in averages, but some extremes are poorly reproduced.
The lack of a specific climate model for each zone means that it is necessary to correct bias to minimize the error between the observation made and the climate model in order to make the statistical distribution of daily data as close as possible to the observed distribution at each point. Figure 1 shows the study area in southwestern Madagascar. It is bounded by latitudes -21° and -26° and longitudes 43° to 46°, included in the blue rectangle.

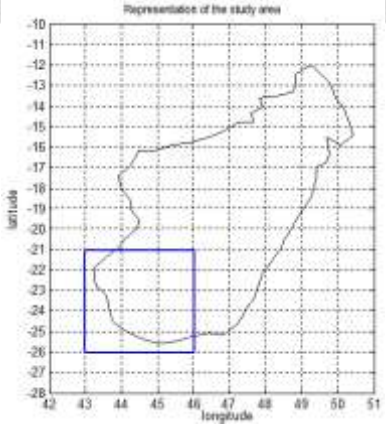

Figure 1: Representation of the study area

2. METHODOLOGIES

2.1 Data

- Temperature data: daily maximum and minimum temperature reanalysis data, spatial resolution 1° x 1° over the period 1985 to 2015, from ECMWF.
- GFDL-GFDL-ESM2M data: these are historical data from 1980 to 2005 for maximum and minimum daily temperatures, as well as data for projections of maximum and minimum daily temperatures from 2006 to 2100, spatial resolution 0.44 ° x 0.44, from the N.O.A.A.

2.2 Methods

The methodology applied is to use:

- the Mann-Kendall test to detect the presence of trends within a time series in the absence of any seasonality or other cycles. The calculated statistic is defined by:

$$S=\sum_{i=1}^{n-1}\sum_{j=i+1}^{n}\operatorname{sgn}\left[\left(y_j-y_i\right)\left(x_j-x_i\right)\right] \text{ where } \operatorname{sgn}(X)=\begin{cases}+1 \text{ if } X>0\\ 0 \text{ if } X=0\\ -1 \text{ if } X<0\end{cases}$$

Mann (1945) and Kendall (1975) demonstrated that:

$$\begin{cases}E(S)=0\\ Var(S)=\dfrac{n(n-1)(2n+5)}{18}\end{cases}$$

If there are ex-aequo in the series, the variance of S is corrected as follows:

$$Var(S)=\frac{1}{18}\left[n(n-1)(2n+5)-\sum_{p=1}^{g}t_p\,(p-1)(2p+5)\right] \text{ where } t_p \text{ is the number of equalities involving p values}$$

As soon as the sample contains about a dozen data, the law of Z-test statistics can be approached by a centered-reduced gaussian.

$$Z=\begin{cases}\dfrac{S-1}{(Var(S))^{\frac{1}{2}}} & \text{if S>0}\\ 0 \text{ si S=0}\\ \dfrac{S+1}{(Var(S))^{\frac{1}{2}}} & \text{if S<0}\end{cases}$$

If we have a sequence of observations $x_1, x_2, \ldots, x_n$ for which we make the two hypotheses:

$$\begin{cases}\text{Hypothesis null } H_0\text{: observations } x_i \text{ are randomly ordered, no trend}\\ \text{Alternative Hypothesis } H_1\text{: Observations } x_i \text{ shows increasing or decreasing trend}\end{cases}$$

The trend of the observation sequence is statistically significant when the p-value of the test is less than 5%. **[1]**

- **Normalized Principal Components Analysis**, which is a factorial dimension reduction method for the statistical exploration of complex quantitative data. This method is widely used in the analysis of climatological data. **[2], [3], [4], [5]**

➢ For two statistical series $k=(x_k, n_k)$ and $h=(x_h, n_h)$ of the same size n with a time depth of several years, the linear correlation coefficient is given by:

$$\boxed{r(k,h)=\frac{1}{n}\sum_{i=1}^{n}\left(\frac{x_{ik}-\bar{x}_k}{s_k}\right)\left(\frac{x_{ih}-\bar{x}_h}{s_h}\right)} \text{ avec } \begin{cases}\bar{x}_k \text{ mean of k}\\ s_k \text{ standard deviation of k}\end{cases} \begin{cases}\bar{x}_h \text{ mean of h}\\ s_h \text{ standard deviation of h}\end{cases}$$

- Data matrix :

Iinitial data table

$$T = \begin{pmatrix} v_{11} & v_{21} & \cdot & \cdot & \cdot & v_{1(p-1)} & v_{1p} \\ v_{21} & v_{22} & \cdot & \cdot & \cdot & v_{2(p-1)} & v_{2p} \\ \cdot & \cdot & \cdot & \cdot & \cdot & \cdot & \cdot \\ \cdot & \cdot & \cdot & \cdot & \cdot & \cdot & \cdot \\ \cdot & \cdot & \cdot & \cdot & \cdot & \cdot & \cdot \\ v_{(n-1)1} & v_{(n-1)2} & \cdot & \cdot & \cdot & v_{(n-1)(p-1)} & v_{(n-1)p} \\ v_{n1} & v_{n2} & \cdot & \cdot & \cdot & v_{n(p-1)} & v_{np} \end{pmatrix}$$

Cloud point center of gravity

$$G = \begin{pmatrix} x_{G1} = \dfrac{\sum_{i=1}^{n} v_{i1}}{n} \\ \cdot \\ \cdot \\ \cdot \\ x_{Gp} = \dfrac{\sum_{i=1}^{n} v_{ip}}{n} \end{pmatrix}$$

Choosing G as the origin leads to the reduced data center table

$$T_{cr} = \begin{pmatrix} \dfrac{v_{11} - x_{G11}}{s_1} & \dfrac{v_{21} - x_{G21}}{s_2} & \cdot \cdot \cdot & \dfrac{v_{1(p-1)} - x_{G1(p-1)}}{s_{(p-1)}} & \dfrac{v_{1p} - x_{G1p}}{s_p} \\ \dfrac{v_{21} - x_{G21}}{s_1} & \dfrac{v_{22} - x_{G22}}{s_2} & \cdot \cdot \cdot & \dfrac{v_{2(p-1)} - x_{G2(p-1)}}{s_{(p-1)}} & \dfrac{v_{2p} - x_{G2p}}{s_p} \\ \cdot & \cdot & \cdot \cdot \cdot & \cdot & \cdot \\ \cdot & \cdot & \cdot \cdot \cdot & \cdot & \cdot \\ \cdot & \cdot & \cdot \cdot \cdot & \cdot & \cdot \\ \dfrac{v_{(n-1)1} - x_{G(n-1)1}}{s_1} & \dfrac{v_{(n-1)2} - x_{G(n-1)2}}{s_2} & \cdot \cdot \cdot & \dfrac{v_{(n-1)(p-1)} - x_{G(n-1)(p-1)}}{s_{(p-1)}} & \dfrac{v_{(n-1)p} - x_{G(n-1)p}}{s_p} \\ \dfrac{v_{n1} - x_{Gn1}}{s_1} & \dfrac{v_{n2} - x_{Gn2}}{s_2} & \cdot \cdot \cdot & \dfrac{v_{n(p-1)} - x_{Gn(p-1)}}{s_{(p-1)}} & \dfrac{v_{np} - x_{Gnp}}{s_p} \end{pmatrix}$$

Reduced centered coordinates of the individual u_i :

$$X_{cri} = \begin{pmatrix} \dfrac{v_{i1} - x_{Gi1}}{s_1} \\ - \\ - \\ - \\ \dfrac{v_{ip} - x_{Gip}}{s_p} \end{pmatrix}$$

Total inertia of the cloud of individuals :

$$I_G = \frac{1}{n}\sum_{i=1}^{n}\sum_{j=1}^{p}\left(\frac{v_{ij} - x_{Gij}}{s_j}\right)^2 = \sum_{j=1}^{p}\left(\frac{1}{n}\sum_{i=1}^{n}\left(\frac{v_{ij} - x_{Gij}}{s_j}\right)^2\right) = \sum_{j=1}^{p}\left(\mathrm{r}\left(v_{ij}\right)\right)$$

Covariance matrix:

$$R = \begin{pmatrix} r(v_{11}) & r(v_{12}) & \cdots & r(v_{1(p-1)}) & r(v_{1p}) \\ r(v_{21}) & r(v_{22}) & \cdots & r(v_{2(p-1)}) & r(v_{2p}) \\ \vdots & \vdots & \cdots & \vdots & \vdots \\ r(v_{(p-1)1}) & r(v_{(p-1)2}) & \cdots & r(v_{(p-1)(p-1)}) & r(v_{(p-1)p}) \\ r(v_{p1}) & r(v_{p2}) & \cdots & r(v_{p(p-1)}) & r(v_{pp}) \end{pmatrix} = \begin{pmatrix} 1 & \cdots & & & \\ \vdots & 1 & \cdots & & \\ & \vdots & 1 & \cdots & \\ & & \vdots & 1 & \cdots \\ & & & \vdots & 1 \end{pmatrix}$$

$$so\ trace(R) = p = I_G$$

- Eigenvalues and eigenvectors :

$$T_{cr}(V) = \lambda V \text{ où } \begin{cases} \lambda \text{ valeur propre} \\ V \text{ vecteur propre} \end{cases}$$

Axes Δ_i passing through G and minimum inertia have for vector director eigenvectors V_i associated with eigenvaluess λ_i such as

$$I_G = \sum_{i=1}^{p} \lambda_i$$

- Selection of the principal axes to be chosen

$$\sum_{i=1}^{p} \lambda_i = p \Rightarrow \bar{\lambda} = \frac{\sum_{i=1}^{p} \lambda_i}{p} = 1 \text{ therefore we can not consider as significant that the } \lambda_i \geq 1$$

By Kaiser's empirical criterion, by centering and reducing the data, we retain the principal components corresponding to eigenvalues greater than 1. **[7]**

- Quality of representation of an individual u_i on an axis Δ_k

The parameter $cos^2\theta$ is used to characterize the quality of representation (qlt) on an axis**. [7], [8], [9]**

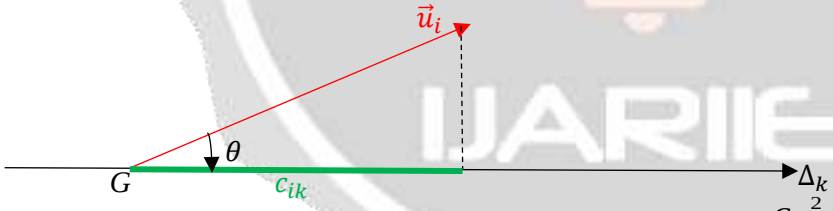

$$qlt_k(u_i) = \cos^2(\theta) = \frac{c_{ik}^2}{\left\|\overrightarrow{Gu_i}\right\|^2}$$

$$\left\|\overrightarrow{Gu_i}\right\|^2 = \sum_{k=1}^{p} c_{ik}^2$$

The closer qlt_i is to 1, the better it is represented.
The closer qlt_i is to 0, the more it is misrepresented.

Quality of representation of variables**. [3], [4], [5]**
On a factorial plane defined by two pricipal axes :

- a variable close to the correlation circle is well represented in this plane;
- a variable close to the origin of the correlation circle is poorly represented in this plane.

- **The Pettitt test**

Statistics of the test:

$$U(t) = \sum_{i=1}^{t} \sum_{j=i+1}^{n} \text{s}\,ign(x_i - x_j)$$

$$T = \max\left\{|U(t)|, t = 1...n\right\}$$

Variant :

$$K = \max\left\{\left|\frac{U(t)}{\sqrt{nt - t^2}}\right|, t = 1...n\right\}$$

Function signs :

$$sign: \ \Re \to \Re$$

$$\forall x \in \Re, \ x \to sign(x) \text{ such as } \begin{cases} \forall x > 0, sign(x) = 1 \\ x = 0, sign(x) = 0 \\ \forall x < 0, sign(x) = -1 \end{cases}$$

The probability p of exceeding the k value taken by the T-statistic of the test on the observed series is given by:

$$p = P(T \geq k) = 2\exp\left(\frac{-6k^2}{T^3 + T^2}\right).$$

If p < α the null hypothesis is rejected. **[8], [9], [10]**

For climatological variables whose time series shows a rupture, it is interesting to calculate the variations on either side of the rupture date by applying the following equation : [**11]**

$$D = \left(\frac{\bar{x}_j}{\bar{x}_i}\right) - 1 \text{ where } \begin{cases} \bar{x}_j \text{ average over the period after rupture} \\ \bar{x}_i \text{ average over the period before rupture} \end{cases}$$

- the **bias correction** by the debinding method, the delta method and the quantile-quantile method: **[12], [13] [14]**
  - debinding method:

$$\begin{cases} B(x,y) = [Mp(x,y,t)] - [O(x,y,t)] \\ Mfc(x,y,t) = Mf(x,y,t) - B(x,y) \\ Mpc(x,y,t) = Mp(x,y,t) - B(x,y) \end{cases} \text{ with } \begin{cases} \text{B : bias} \\ \text{O: observation} \\ \text{M : model} \\ \text{p : present} \\ \text{f : future} \\ \text{c : corrected} \\ [\ ] : \text{climatological mean} \end{cases}$$

  - delta method :

$$\begin{cases} Delta(x,y) = \left[M_f(x,y,t)\right] - \left[M_p(x,y,t)\right] \\ M_{fc}(x,y,t) = O(x,y,t) + Delta(x,y) \end{cases} \text{ avec } \begin{cases} O: \text{ observation} \\ \text{M : model} \\ \text{p : present} \\ \text{f : future} \\ \text{c : corrected} \\ [\ ] : \text{climatological mean} \end{cases}$$

  - Quantile-quantile method :

The order quantiles of 0.01% to 99.9% of the daily values of the simulation considered and the observations are calculated, taking into account the same learning period.

In a point i of the grid and for each order k of quantile, we calculate the correction coefficient $Corr^k(i)$ given by :

$$Corr^k(i) = \begin{cases} 0 \ si \ Q^k(i) = 0 \\ \dfrac{Q_{obs}{}^k(i)}{Q^k(i)} \ si \ Q^k(i) \neq 0 \end{cases} \text{ with } \begin{cases} Q^k(i): value\ at\ point\ i\ of\ the\ quantile\ simulated\ model\ of\ order\ k \\ Q_{obs}{}^k(i): value\ of\ the\ corresponding\ observation\ quantile \end{cases}$$

For each day j of the period and in a point i of the grid of the observations data, we look for the order k of the model quantile (interpolated) directly inferior to the value of the daily O(j, i) of day j at the point i:

$$k = \begin{cases} 0,999 \text{ if } O(j,i) \geq Q^{0.999}(i) \\ otherwise\ k\ is\ such\ that\ Q^{k}(i) \leq O(j,i) < Q^{k+1}(i) \end{cases}$$

The corrected value of day j at point i, is given by the formula :

$$M_c(j,i) = O(j,i) * Corr^k(i)$$

3. RESULTS AND DISCUSSIONS

3.1 Spatial distribution of maximum and minimum temperatures in the study area

Figure 2-a (left) shows the spatial distribution of the daily average value of the maximum temperature. The black lines represent the isotherms. This maximum temperature decreases progressively as one moves away from the latitude point -24° and longitude 44°. Its maximum value of 30°C shall be observed on either side of longitude 44° and between latitudes -25.75° and -22.75°. North and east of the study area, the maximum temperature is 25°C.

Figure 2-b (right) shows the spatial distribution of the daily average minimum temperature. The black lines represent the isotherms. This minimum temperature increases progressively as one moves away from the latiude point -24° and longitude 46° where its value is close to 17°C. The maximum value of 25 °C is observed in the maritime part in the extreme south-east.

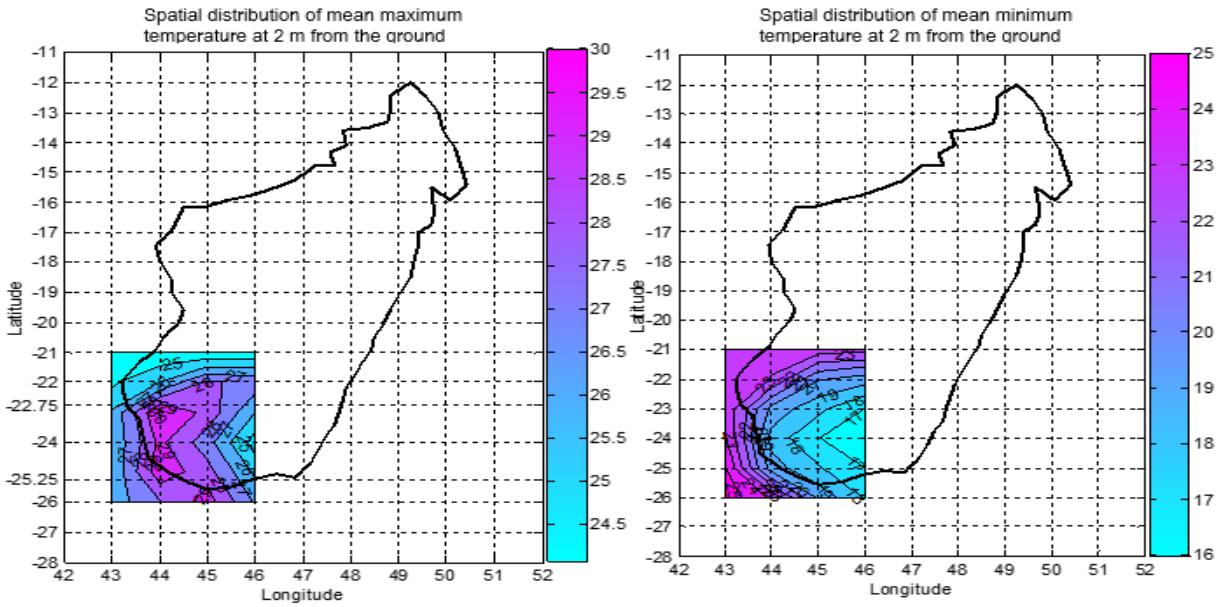

Figure 2-a **Figure 2-b**

Figure 2 : Spatial distribution of maximum and minimum daily mean temperatures in the study area

3.2 Climatological mean of temperature from 1985 to 2015 in the study area

Figure 3 shows the daily and monthly climatological mean curves in the study area. The red and blue curves are the climatological means of minimum temperature and the climatological means of maximum temperature over the study period, respectively.

The maximum monthly climatological mean of maximum temperature is 28.26°C (maximum temperature mean of the months of November) and its minimum is 23.51°C (maximum temperature mean of the months of July).

The maximum monthly climatological mean of minimum temperature is 23.86°C (minimum temperature mean of the months of February) and its minimum is 17.24°C (minimum temperature mean of the months of July).

The maximum of the daily climatological mean of maximum temperature is 29,05 °C (maximum temperatures mean on November 14) and its minimum is 23,11 °C (maximum temperatures mean on July 7).
The maximum daily climatological mean of minimum temperature is 24.16°C (minimum temperatures mean on January 27) and its minimum is 16.87 °C (minimum temperatures mean on July 8).

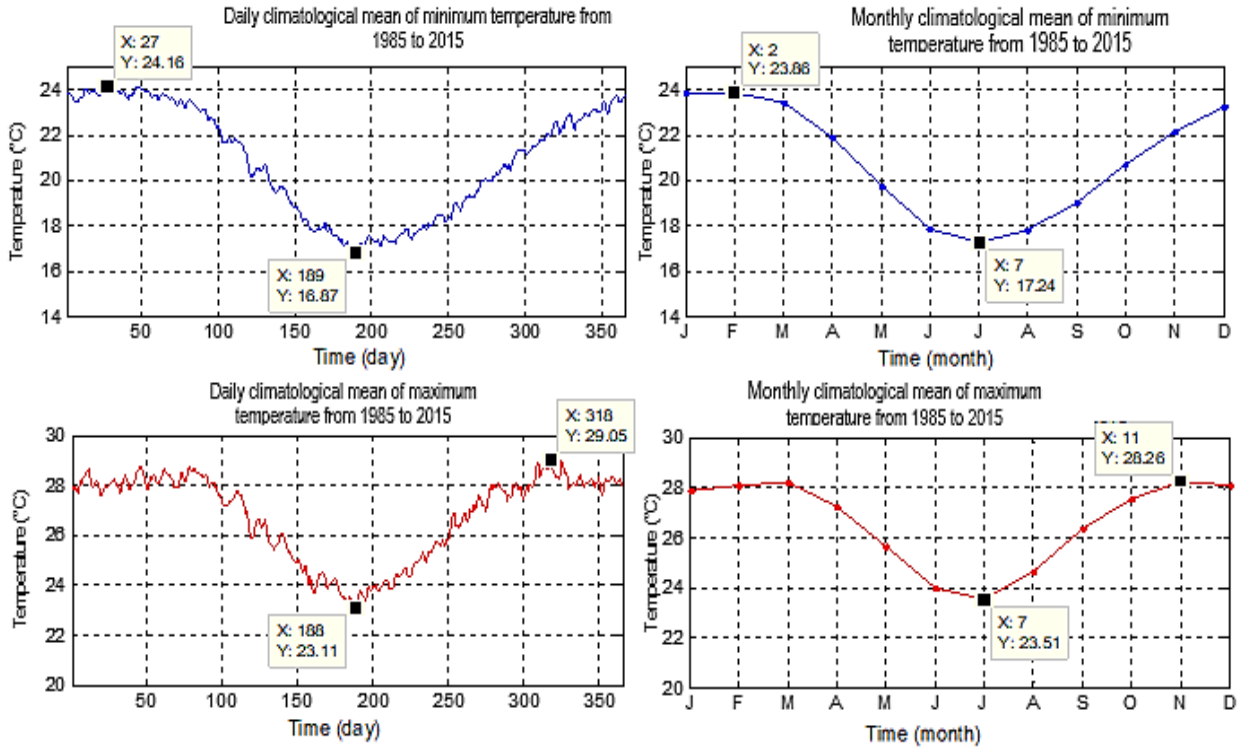

Figure 3: Variation in daily and monthly climatological mean of maximum and minimum temperatures

3.3 Evolution of annual mean temperatures from 1985 to 2015

Figure 4 shows the evolution of the minimum annual mean temperature and that of the maximum annual mean temperature.
The line in blue represents the trend of evolution for the maximum temperature. It is of equation $y = 0.022x + 26.279$ where the origin is the year 1985. The slope being positive therefore the minimum temperature has a tendency to increase of 0,022 ° C / year. The Mann Kendall test gives a p-value equal to 0.0089. As this value is well below 0.05, the trend is significant.
The purple line represents the trend of the evolution for the minimum temperature, with equation $y = 0.012x + 20.725$. It is of positive slope so the minimum temperature also has an upward trend of 0.012°C/year but the value of the p-value is equal to 0.0527, which is greater than 0.05, so this trend is not significant.

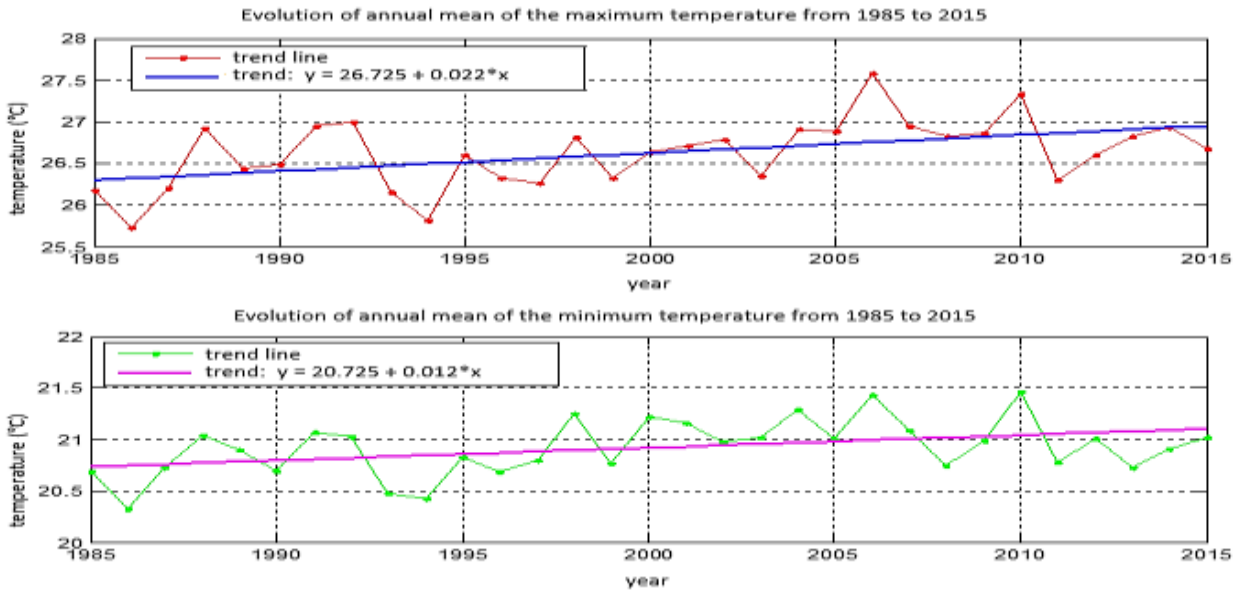

Figure 4 : Curves and trend lines of annual mean of maximum and minimum temperatures

3.4 Annual anomaly of maximum and minimum temperature from 1985 to 2015

The moving average curve of the annual anomaly is increasing for both temperatures from negative to positive. There was generally a predominance of 2 distinct periods in the time series : at first a relatively cool period (negative anomaly) and then an increasingly hot period (positive anomaly). (**Figure 5**)

With a few exceptions : the annual anomaly of the maximum temperature is deficit from 1985 to 1999. The minimum value of -0.893 ° C observed in 1986. From the year 2000 this annual anomaly is in excess. The maximum value of 0.96 ° C observed in 2010.

With a few exceptions : the annual anomaly of the minimum temperature is in deficit from 1985 to 1997. The minimum value of -0.598°C is observed in 1986. From 1998 onwards this annual anomaly is excessive. The maximum value is 0.544°C observed in 2010.

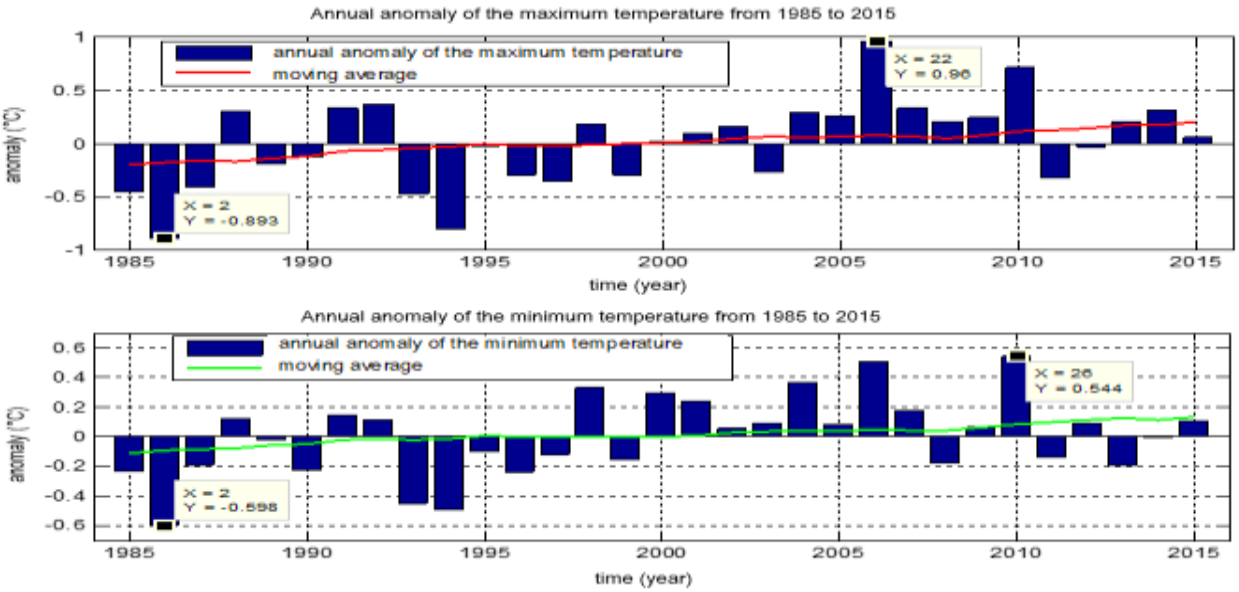

Figure 5 : annual anomaly of maximum and minimum temperatures from 1985 to 2015

3.5 Observation of climate change in the study area

La **Figure 6** représente les courbes du test de Pettitt appliqué aux températures maximale et minimale sur la période 1985-2015. La courbe à gauche atteint son maximum à l'année 2003 : c'est l'année de rupture pour la température maximale. La courbe à droite atteint son maximum à l'année 1997 : c'est l'année de rupture pour la température minimale.

Figure 6 shows the curves of the Pettitt test applied at maximum and minimum temperatures over the period 1985-2015. The curve on the left reaches its maximum in the year 2003: it is the year of rupture for the maximum temperature. The curve on the right reaches its maximum in 1997: it is the year of rupture for the minimum temperature.

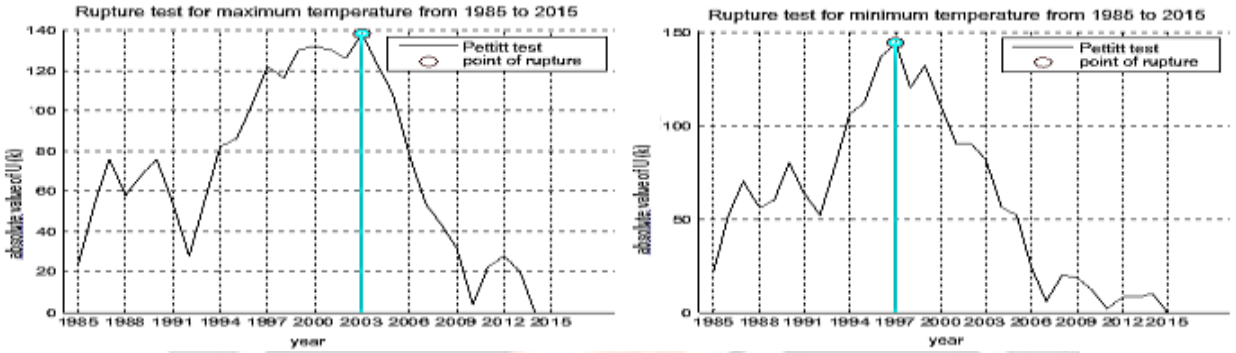

Figure 6 : Pettitt rupture test for maximum and minimum temperatures

Indeed, over the period 1997-1998 El Nino caused a natural disaster in the world. Some countries have suffered from drought while others have experienced abnormally heavy precipitation **[15]**. This phenomenon did not spare our study area and left an immediate consequence on the increase in the minimum temperature as shown in **Table 1**. This increase is quite alarming compared to the increase in the global average temperature which seems to increase by 0,85°C since 1880. **[16]**

Table 1: Variation in mean maximum and minimum temperatures

Climate variable	Mean before date of rupture	Date of rupture	Mean after date of rupture	Increase
Minimal temperature	20,74 °C	1997	20,92 °C	0,18 °C
Maximal temperature	26,40 °C	2003	26,63 °C	0,23 °C

3.6 Principal Components Analysis results

In Principal Components Analysis, all the temperatures at each point of intersection of latitude and longitude in the area at the spatial resolution of 1 ° x 1 ° were selected as individuals and the 12 months of 'year. This gives 6 points according to the latitude and 4 points according to the longitude. Therefore, there are 24 points of intersections representing the individuals. **(Figure 7)**

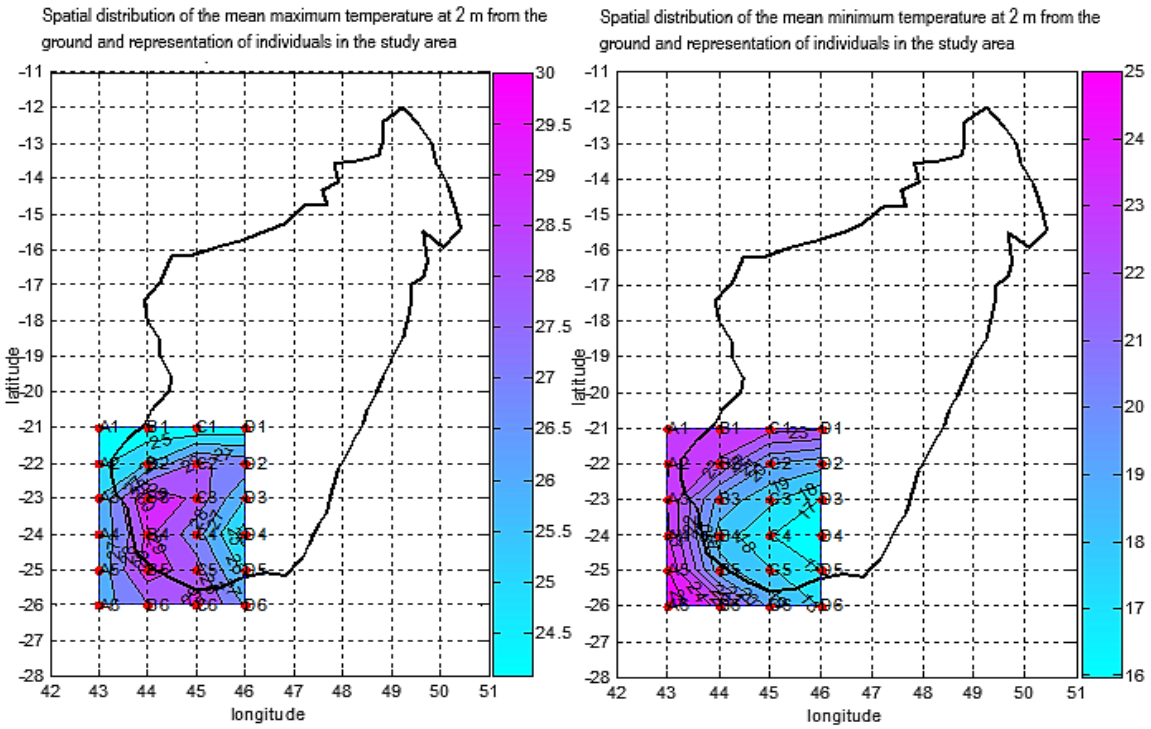

Figure 7 : representation of individuals in the study area

3.6.1 Choice of number of axes to choose

The Kaiser criterion and the elbow criterion allow to keep the factorial axes F1 and F2 explaining more than 84% of the total inertia of the cloud, to study the behaviour of each individual in relation to the others.

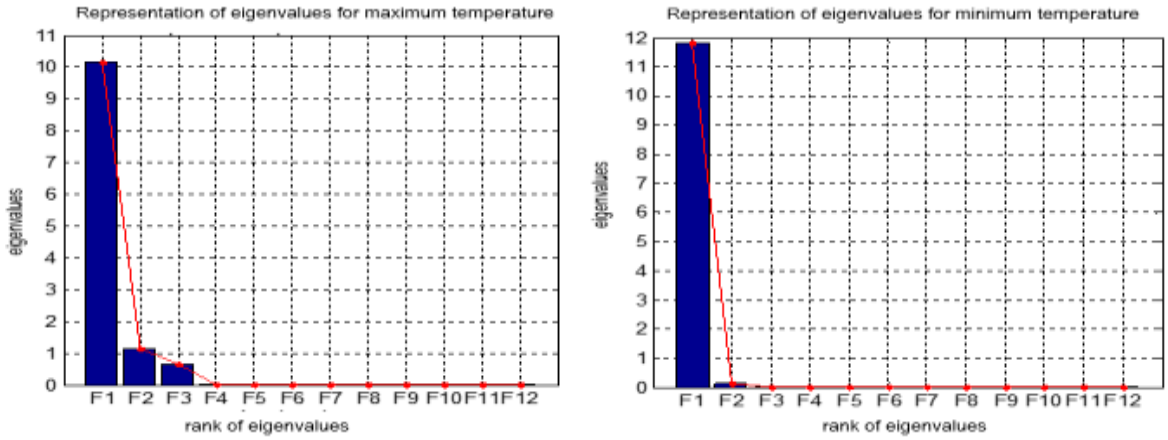

Figure 8 : representation of eigenvalues for maximum and minimum temperatures

3.6.2 Projections of variables and individuals on factorial plan F1-F2

Figure 9 shows the projection of the variables in the factor plane F1-F2. The variables April, March, August, September, October and November are very well represented in this factor plan for maximum temperature. Every month is well represented for the minimum temperature in the factor plan F1-F2.

All variables are positively correlated with the F1 axis for both maximum and minimum temperatures.

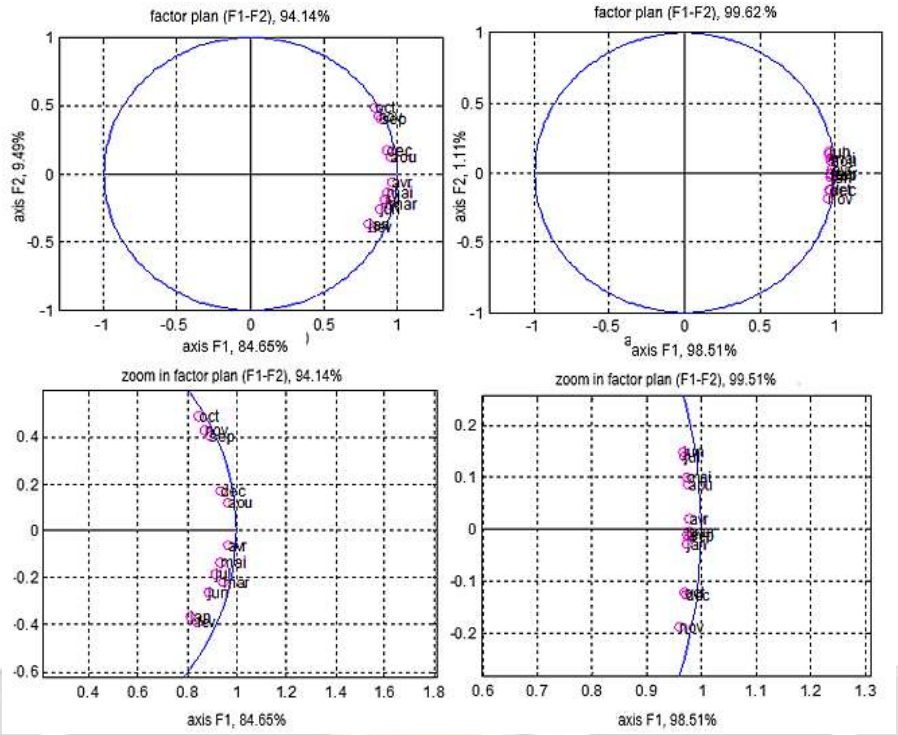

Figure 9 : projection of variables on factor plane F1-F2 for maximum and minimum temperature

3.6.3 Projections of the individuals

The axis F1 in Figure 10, which explains more than 84% of total inertia, is interpreted as follows :

- for the maximum temperature :

the individual B4 contributes the most to the construction of the F1 axis and this axis opposes the individual B4 to D3. In Figure 7, individual B4 is on a grid point of the warmest average temperature 30°C and D3 on isotherm 26°C in the relatively cold part of the zone. Given the correlation circle in Figure 9, the month of April is very well represented on the F1 axis which is a hot month according to Figure 3. As a first approximation, the F1 axis therefore orders individuals according to their increasing maximum temperature.

- for the minimum temperature:

the individual D3 contributes the most to the construction of the axis F1 and this axis opposes the individual D3 to A1. In Figure 7, individual D3 is on the average 17°C isotherm which is in the relatively cold part and A1 in the relatively hot part of the zone. Given the correlation circle in Figure 9, the month of April is also well represented on the axis F1 which is a hot month according to Figure 3. As a first approximation, the axis F1 therefore orders individuals according to their increasing minimum temperature.

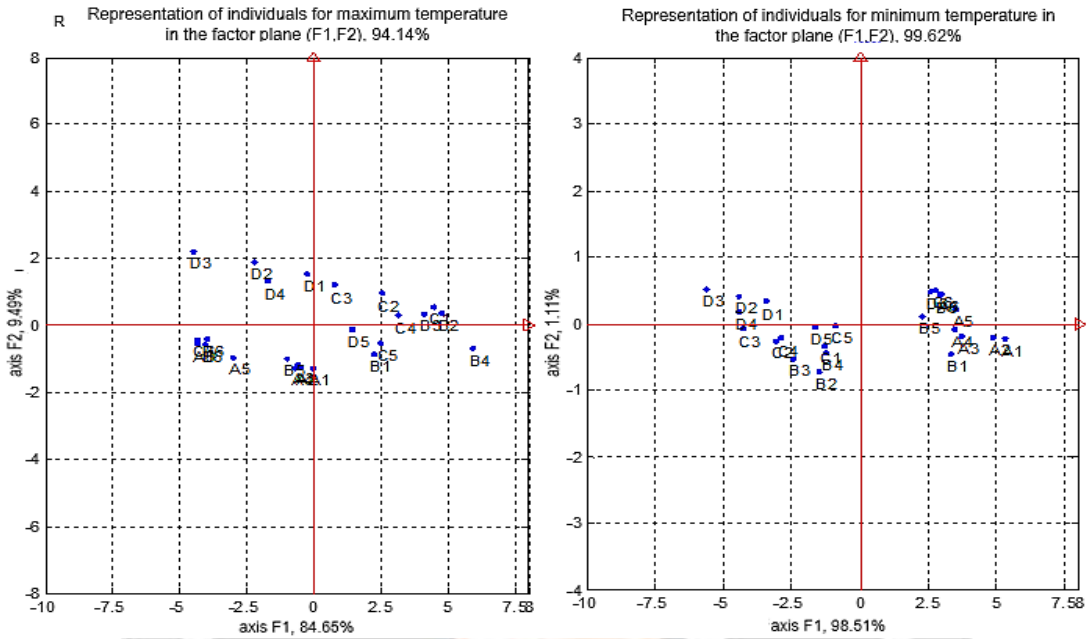

Figure 10 : projection of individuals on factor plane F1-F2 for maximum and minimum temperatures

3.6.4 Regionalization of the study area

Taking into account the relationship between individuals and variables, the study area can be subdivided as follows : **(Figure 11)**

- for maximum temperature, in 5 different regions according to their provisions for the F1 axis which provides 84.65% of total inertia:

region 1 : consists of **B4** (in red) . This area is very hot most of the year.

region 2 : consisting of **C3**, **C2**, **C4**, **C1**, **B2**, and **B3** (in purple). These areas are very hot during the southern summer, except in January and February.

region 3 : consists of **B1**, **C5** and **D5** (in yellow). These areas are characterized by moderately warm temperatures during the southern winter and even in the southern summer in January and February.

region 4 : constituée de **A1**, **A2**, **A3**, **A4**, **A5**, **A6**, **B5**, **B6**, **C6**, **D6** (en vert) . Ces zones sont moyennement chaude pendant toute l'année
consists of **A1**, **A2**, **A3**, **A4**, **A5**, **A6**, **B5**, **B6**, **C6** and **D6** (in green). These areas are moderately warm throughout the year.

region 5 : consists of **D1**, **D2**, **D3**, and **D4** (sky blue). In these areas, the temperature is cool during the southern summer except for January and February.

- for the minimum temperature, in 3 different regions according to their provisions regarding the axis F1 which provides 98.51% of the total inertia :

region 1 : consisting of **A1**, **A2**, **A3**, **A4**, **A5**, **A6**, **B1**, **B5**, **B6**, **C6** and **D6** (in red). These areas are characterized by relatively high minimum temperature.

region 2 : consisting of **B2**, **B3**, **B4**, **C1**, **C2**, **C4**, **C5**, and **D5** (in yellow). These areas are characterized by cool minimum temperature.

region 3 : consisting of **C3**, **D1**, **D2**, **D3**, and **D4** (in blue). These are mountainous areas, characterized by relatively cold temperatures.

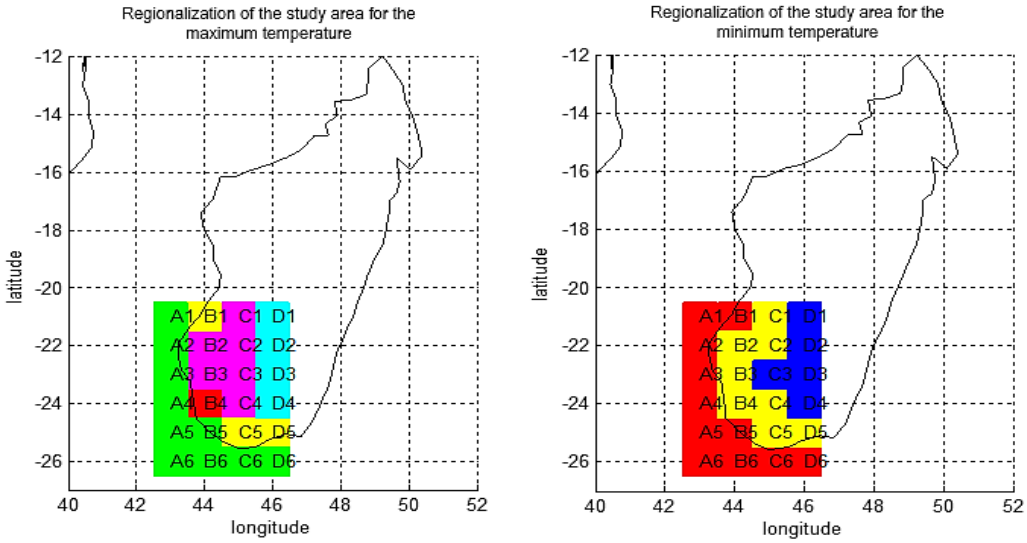

Figure 11 : distribution of regions with similar maximum and minimum temperatures

3.7 Bias correction of the NOAA GFDL-GFDL-ESM2M climate model under the RCP4.5 and RCP8.5 scenarios

3.7.1 Maximum temperature bias correction and appropriate method selection

The most suitable method of correction is the one whose average difference between its result and the observation is minimal in absolute value.

- **Figure 12** shows the bias corrections of the NOAA GFDL-GFDL-ESM2M climate model under RCP4.5 scenarios in regions 1-5 by the debinding method, the delta method and the quantile-quantile method for the maximum temperature.

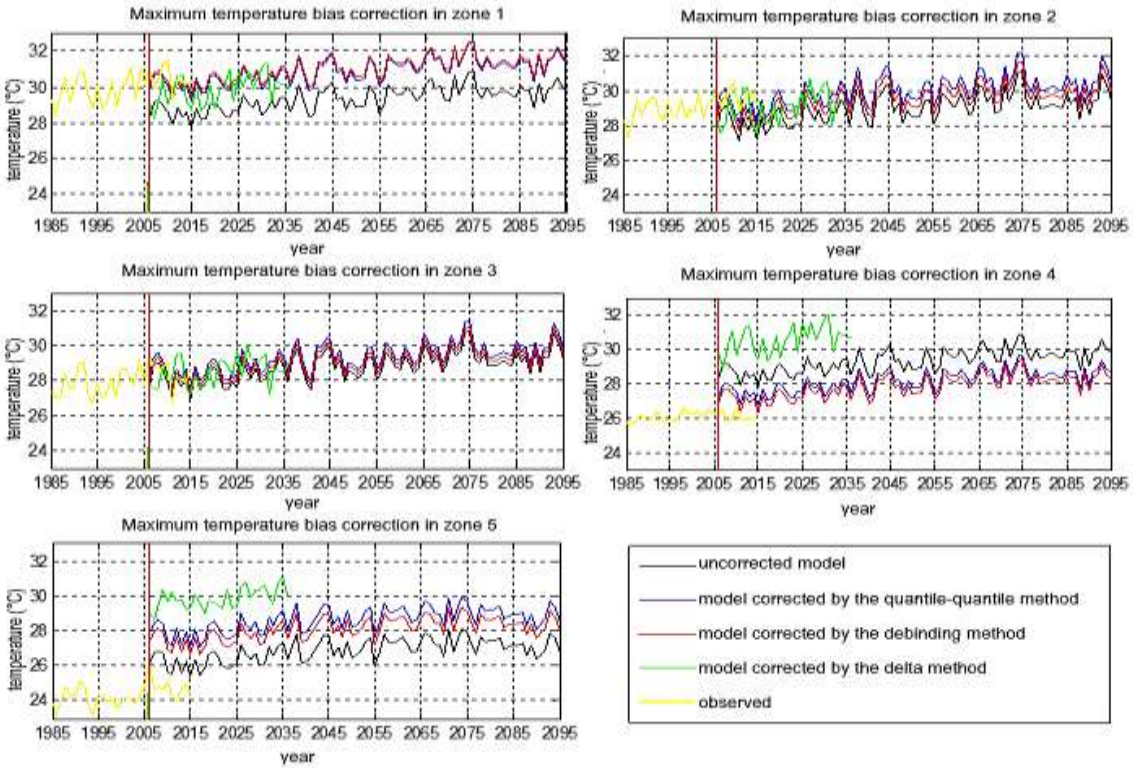

Figure 12 : Correction of the NOAA GFDL-GFDL-ESM2M climate model under the RCP4.5 scenario for maximum temperature

Table 2 summarizes the average difference between the result of each correction method and the observation. **Table 2** shows the most suitable method for each region.

Table 2 : Mean difference between the result of each correction method and the observation

Regions	**Average deviations from observation over the 2005-2015 validation period**			**Adapted correction method**
	debinding	**quantile-quantile**	**delta**	
Region 1	**0.0237**	0.0425	0.0943	debinding method
Region 2	0.0913	**0.0510**	0.0923	quantile-quantile method
Region 3	0.0181	**-0.0061**	0.0292	quantile-quantile method
Region 4	**-0.0998**	-0.1353	-0.4114	debinding method
Region 5	**-0.2610**	-0.3078	-0.4773	debinding method

- **Figure 13** shows the corrections of the NOAA GFDL-GFDL-ESM2M climate model under RCP8.5 scenarios in Regions 1-5 by the debinding method, the delta method and the quantile-quantile method for maximum temperature.

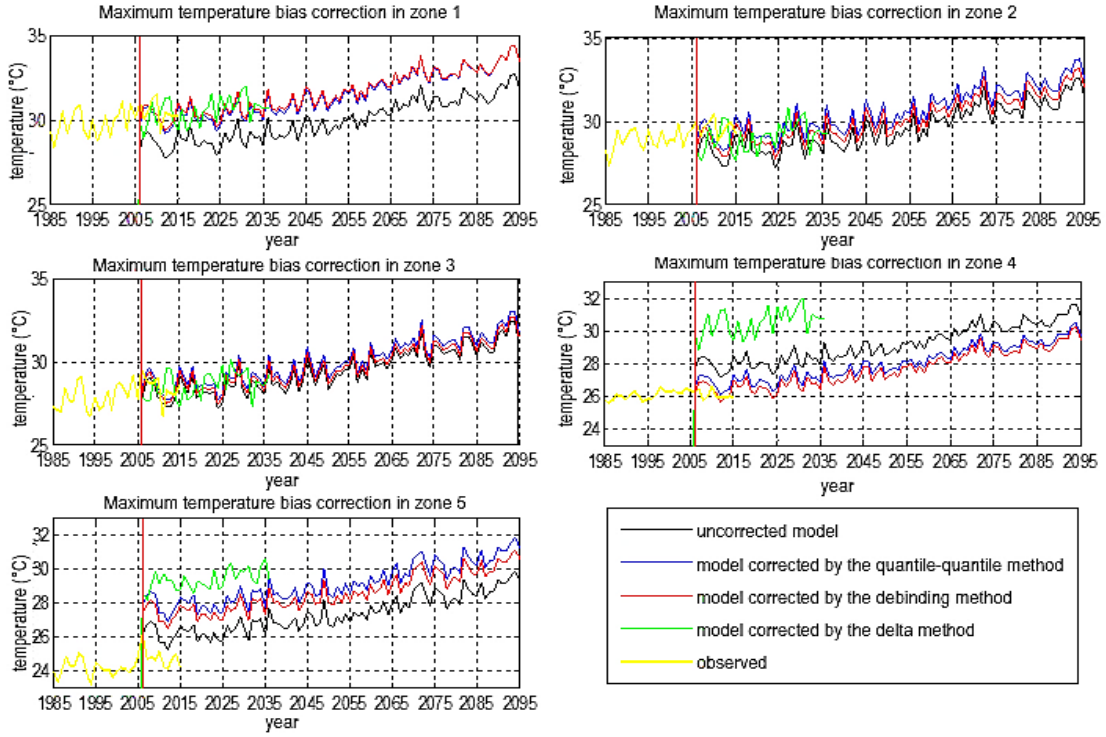

Figure 13 : Correction of the NOAA GFDL-GFDL-ESM2M climate model under the RCP8.5 scenario for maximum temperature

Table 3 summarizes the average difference between the result of each correction method and the observation. **Table 3** shows the most suitable method for each region.

Table 3: Mean difference between result of each correction method and observation

Regions	**Average deviations from observation over the 2005-2015 validation period**			**Adapted correction method**
	debinding	**quantile-quantile**	**delta**	
Region 1	**0.0230**	0.0418	0.0306	debinding method
Region 2	0.0818	**0.0411**	0.0897	quantile-quantile method
Region 3	**0.0060**	-0.0185	0.0213	debinding method
Region 4	**-0.0319**	-0.0700	-0.4066	debinding method
Region 5	**-0.2633**	-0.3103	-0.4308	debinding method

3.7.2 Correction of minimum temperature bias

- **Figure 14** shows the bias corrections of the NOAA GFDL-GFDL-ESM2M climate model under RCP4.5 scenarios in regions 1-5 by the debinding method, the delta method and the quantile-quantile method of minimum temperature.

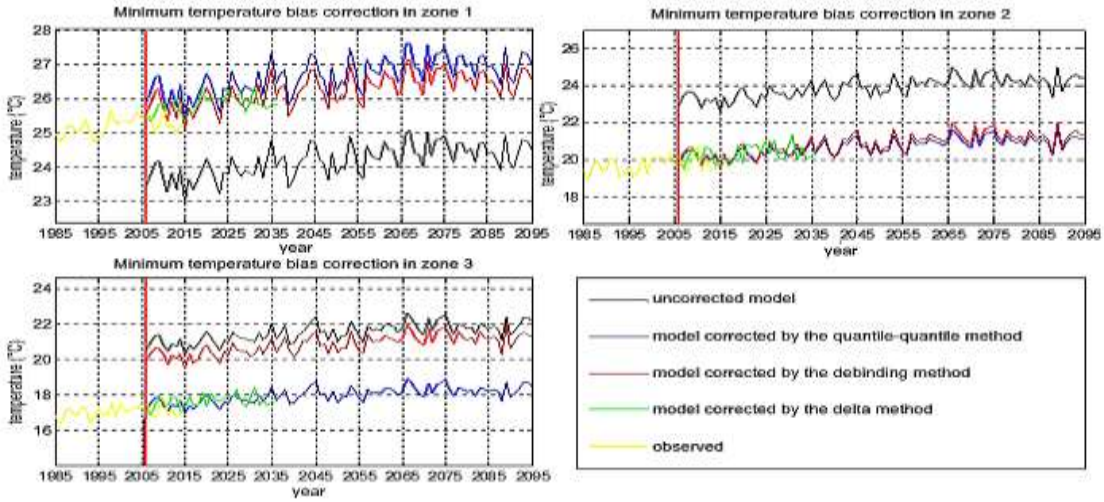

Figure 14 : Correction of the NOAA GFDL-GFDL-ESM2M climate model under the RCP4.5 scenario for minimum temperature

Table 4 summarizes the average difference between the result of each correction method and the observation. This Table 4 demonstrates which of these methods is best suited for each region.

Tableau 4 : écart moyenne entre résultat de chaque méthode de correction et l'observation

Regions	**Average deviations from observation over the 2005-2015 validation period**			**Adapted correction method**
	debinding	**quantile-quantile**	**delta**	
Region 1	-0.0468	-0.0819	**-0.0383**	delta method
Region 2	-0.0333	**-0.0254**	-0.0283	quantile-quantile method
Region 3	-0.3015	**-0.0298**	-0.0325	quantile-quantile method

- **Figure 15** shows the corrections of the NOAA GFDL-GFDL-ESM2M climate model under RCP 8.5 scenarios in Regions 1-5 by the debinding method, the delta method and the quantile-quantile method for the minimum temperature.

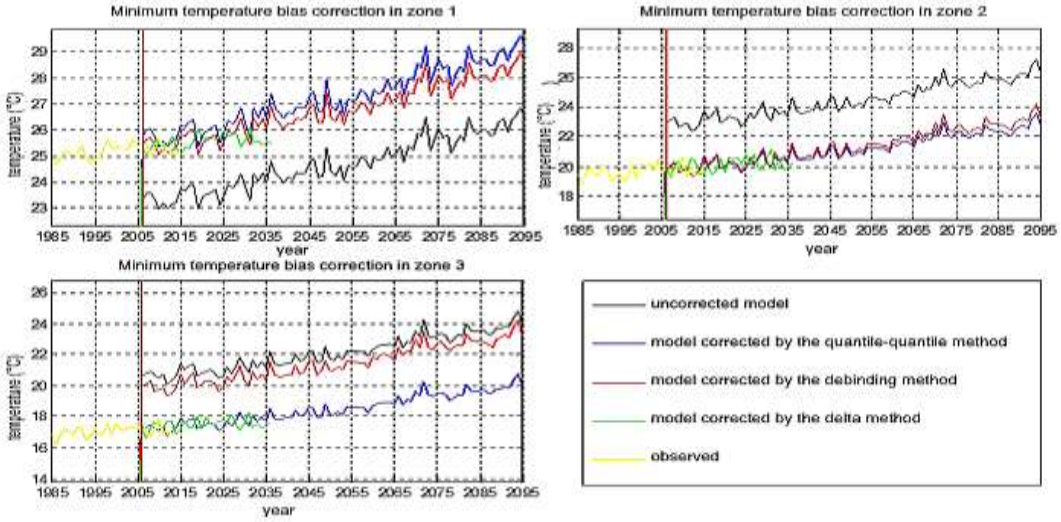

Figure 15 : Correction of the NOAA GFDL-GFDL-ESM2M climate model under the RCP8.5 scenario for minimum temperature

Table 5 summarizes the average difference between the result of each correction method and the observation. **Table 5** reveals the best method for each of these regions

Table 5: Mean difference between result of each correction method and observation

Regions	**Average deviations from observation over the 2005-2015 validation period**			**Adapted correction method**
	debinding	**quantile-quantile**	**delta**	
Region 1	**-0.0136**	-0.0453	-0.0113	delta method
Region 2	-0.0070	**-0.0027**	-0.0091	quantile-quantile method
Region 3	-0.2752	**-0.0130**	-0.0172	quantile-quantile method

4. CONCLUSIONS

In this article, we carried out the study of temperatures followed by bias correction of the climate model GFDL-GFDL-ESM2M of the National Oceanographic and Administration in the South-West region of Madagascar, bounded by latitudes -21° to -26° and longitudes 43° to 46°. This study is based on maximum and minimum temperature reanalysis data from the ECMWF during the period 1985 to 2015, over a period of 31 years of observations.

The study of the evolution of the annual average temperature showed that the maximum temperature has an upward trend of 0.022°C per year. This trend is significant according to the Mann Kendall test which gives a p-value equal to 0.0089. With a few exceptions, the anomaly of the maximum temperature is in deficit from 1985 to 1999 and is in excess from the year 2000. But the Pettitt test shows that the year of rupture is in 2003 with an increase of 0.23 ° C.

The result of the Principal Component Analysis showed the existence of:

- five regions with the same climatic conditions relative to the maximum temperature:

region 1 : it is a very hot area almost all year round.
region 2 : this region is very hot during the southern summer, except in January and February.
region 3 : It is characterized by a moderately warm temperature during the southern winter and even in the southern summer in January and February.
region 4 : this region is moderately warm throughout the year
region 5 : in these regions the temperature is cool during the southern summer except for January and February.

- three regions with the same climatic conditions relative to the minimum temperature:

region 1 : this region is characterized by a relatively high minimum temperature.
region 2 : in this region the minimum temperature is cool.
region 3 : It is a mountainous region, characterized by relatively cold temperatures.

The bias correction of the NOAA GFDL-GFDL-ESM2M climate model under the RCP4.5 and RCP8.5 scenarios was done in each region:

- The bias correction of the model for maximum temperature showed that:
  - ➢ the debinding method is suitable for:
  - Region 1, Region 4 and Region 5 under the RCP4.5 scenario;
  - Region 1, Region 3, Region 4 and Region 5 under the RCP8.5 scenario;
  - ➢ the quantile-quantile method is suitable for:
  - Region 2 and Region 3 under the RCP4.5 scenario;
  - Region 2 under the RCP8.5 scenario;
- the model bias correction for the minimum temperature showed that:
  - ➢ the quantile-quantile method is suitable for:
  - Region 2 and Region 3 under scenario RCP4.5 and RCP8.5;
  - ➢ the delta method is suitable for:
  - Region 1 under scenario RCP4.5 and RCP8.5;

5. REFERENCES

[1] N. Croiset, B. Lopez (BRGM), Outil d'analyse statistique des séries temporelles d'évolution de la qualité des eaux souterraines, Manuel d'utilisation, Rapport final, pp.18-19

[2] P. Besse www.math. univ-toulouse.fr/besse, M2 MASS, TP4 : Introduction au logiciel SAS Procédures statistiques multivariées : Analyse en Composantes Principales. Pages 1, 2.

[3] C.DUBY, S ROBIN ; Analyse composantes principale, juillet 2006. Pages 4,5.

[4] Aimé KOUDOU et al, CONTRIBUTION DE L'ANALYSE EN COMPOSANTES PRINCIPALES A LA REGIONALISATION DES PLUIES DU BSSIN VERSANT DU N'ZI, CENTRE DE LA COTE D'IVOIRE, 2015. Page 162.

[5] Ali Kouani, S. El Jamali et M.Talbi, Analyse en Composantes principales, Une méthode factorielle pour traiter les données didactique, février 2007. Page 3.

[6] ADD3-MAB, D-interpretation d'une ACP, 2011.Papes 4, 29.

[7] Jean-Marc Labatte, jean-marc.Labatte@univ-angers.fr, Analyse des données M2, consulté le 17 Février 2017.

[8] Lemaitre Fabien, Travail de fin d'étude, juin 2002. Page 12.

[9] Cheikh FAYE, impact du changement climatique et du barrage de Manantali sur la dynamique du régime hydrologique du fleuve Sénégal à Bakel, 2015 ou cheikh.faye@univ-zig.sn, consulté le 24 Novembre 2017.

[10] Thorsten Pohlert, Non-Parametric Trend Test and change-Point Détection Novembre 12,2017. Page 10.

[11] Tanina. D. SORO, Nagnin SORO, 2011: Variabilité climatique et son impact sur les ressources en eau dans le dégré carrré de grand-lahou (Sud-Ouest de la cote d'ivoire). Pages 125, 131.

[12] Julien Boé : Désagrégation spatiale : les différentes approches avec des applications dans l'étude des impacts du changement climatique, 26 Septembre 2014. Page 25.

[13] Frédéric HUARD, INRA Agro Clim, Régionalisation statistique pour les études d'impact du changement climatique : pourquoi et comment. Pages 7, 8, 9, 10.

[14] Jeanne Colin, 20 Juin 2011, Étude des évènements précipitants intenses en méditerrané : Approche par la modélisation climatique régionale, Thèse de doctorat en climatologie, Université de Toulouse, p125.

[15] OMM, les catastrophes ; impact socioéconomique du phénomène EL Nino 1997-1998, 1999 ; UNU, 2001. Pages 272, 273.

[16] http://www.climatechallenge.be/fr/des-infos-en-mots-et-en-images/le-changement-climatique/les-hommes-et-le-climat/augmentation-de-la-temperature-globale.aspx , consulté le 2 septembre 2018